



Fluorescence properties of novel near-infrared phosphor $\text{CaSc}_2\text{O}_4:\text{Ce}^{3+}, \text{Nd}^{3+}$

J.X. Meng^{a,b,*}, F.J. Zhang^a, W.F. Peng^a, W.J. Wan^a, Q.L. Xiao^a, Q.Q. Chen^a, L.W. Cao^a, Z.L. Wang^c

^a Department of Chemistry, Jinan University, Guangzhou 510632, China

^b Institute of Nanochemistry, Jinan University, Guangzhou 510632, China

^c School of Chemistry and Biotechnology, Yunnan Nationalities University, Kunming 650031, China

ARTICLE INFO

Article history:

Received 23 December 2009

Received in revised form 8 August 2010

Accepted 16 August 2010

Available online 26 August 2010

Keywords:

Rare earth compounds

Co-precipitation methods

Near-infrared luminescence

Energy transfer

Sensitization

ABSTRACT

Novel near-infrared (NIR) phosphor, $\text{CaSc}_2\text{O}_4:\text{Ce}^{3+}, \text{Nd}^{3+}$, was synthesized by co-precipitation method followed by firing at 1300 °C in reduced atmosphere. When irradiated with blue light, the phosphor gives strong Nd^{3+} characteristic NIR emissions in the range of 880–930 nm. The NIR emission intensity gets a 200 times enhancement by co-doping of Ce^{3+} . Detailed investigation on spectrum and fluorescence lifetimes indicated the NIR luminescence enhancement is obtained from an energy transfer process. The process initiates with efficient absorption of blue light by Ce^{3+} ions via an allowed 4f–5d transition, follow by efficient energy transfer from Ce^{3+} to Nd^{3+} , and emitting strong Nd^{3+} characteristic fluorescence.

© 2010 Elsevier B.V. All rights reserved.

1. Introduction

Efficient near-infrared (NIR) luminescent lanthanide materials, with unique narrow line width and long lifetime, have drawn great attentions in recent years. They have been successively applied in fiber optical communication [1], solid-state laser [2] and fluoroimmunoassay [3]. Nd^{3+} , Yb^{3+} and Er^{3+} are the most frequently reported NIR luminescent lanthanide ions (Ln^{3+}). However, NIR photoluminescence of Ln^{3+} is relatively weak compared with their visible counterparts. Since the emission energy levels of NIR luminescent Ln^{3+} is remarkably lower than their visible counterparts, NIR luminescence of Ln^{3+} can be quenched much more efficiently via phonon or collision with surrounding atoms. These facts could partly explain the low efficiency of NIR luminescence of Ln^{3+} . Another more important reason is their low excitation efficiency. Luminescence of Ln^{3+} usually originates from transitions within the partially filled 4f levels, which are in principle spin-forbidden, and usually with low direct excitation efficiency (extinction coefficient are typically $1 \times 10^{-10} \text{ M}^{-1} \text{ cm}^{-1}$) and very long lifetime (typically in the range from several microseconds to several milliseconds). Consequently, direct excitation of the f–f transition of Ln^{3+} is normally inefficient.

Most efficient Ln^{3+} f–f fluorescence involved an energy transfer process. For example, “antenna” effects have been extensively reported in many Ln^{3+} complexes [2,4–12], in which an organic ligand with large extinction coefficient was always involved to absorb light and be excited to its higher energy levels, and then transfer energy to the center Ln^{3+} ions to give sensitized f–f emission. This “antenna” effect has been demonstrated to be effective in organic complexes of both visible luminescent Ln^{3+} ($\text{Ln}^{3+} = \text{Tb}^{3+}, \text{Eu}^{3+}, \text{Sm}^{3+}$) [4,5,13–17] and NIR luminescent Ln^{3+} ($\text{Ln}^{3+} = \text{Tb}^{3+}, \text{Eu}^{3+}, \text{Sm}^{3+}$) [4,5,13,18]. For Ln^{3+} luminescent materials in inorganic matrix, energy transfer from a moiety with large extinction coefficient to Ln^{3+} have also been shown to be essential to achieve an excellent Ln^{3+} luminescence, such as energy transfer from VO_4 moiety to Eu^{3+} in $\text{YVO}_4:\text{Eu}$ [19] and energy transfer from Ce^{3+} to Tb^{3+} in $\text{LaPO}_4:\text{Ce}^{3+}, \text{Tb}^{3+}$ [20]. However, reports on this type of energy transfer in NIR luminescent materials are sparse. Recently, we reported that NIR luminescence of Er^{3+} or Nd^{3+} in yttrium aluminum garnet (YAG) could be very efficiently sensitized via an energy transfer from co-doping Ce^{3+} [6,7]. These results indicated the possibilities of observing sensitized NIR luminescence in other matrix in which the luminescence properties of co-doping Ce^{3+} is similar to that in YAG. In the present work, $\text{Ce}^{3+}/\text{Nd}^{3+}$ co-doped CaSc_2O_4 with efficient NIR luminescence was synthesized by a co-precipitation method. It was found that $\text{CaSc}_2\text{O}_4:\text{Ce}^{3+}, \text{Nd}^{3+}$ can give efficient Nd^{3+} characteristic NIR luminescence when excited with a blue light. The effects of $\text{Ce}^{3+}/\text{Nd}^{3+}$ doping concentration on the NIR emission properties were also investigated. Mechanism for the energy transfer from Ce^{3+} to Nd^{3+} was also briefly discussed.

* Corresponding author at: Department of Chemistry, Jinan University, Guangzhou 510632, China. Tel.: +86 20 85220223; fax: +86 20 85221697.
E-mail address: tmjx@jnu.edu.cn (J.X. Meng).

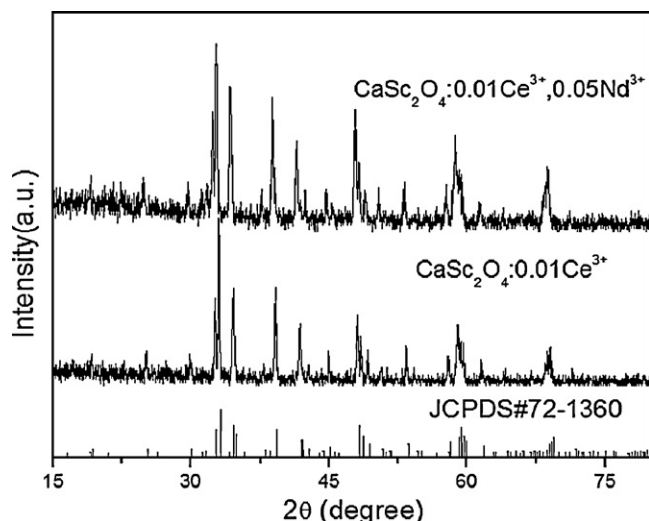


Fig. 1. XRD patterns of $\text{CaSc}_2\text{O}_4:\text{Ce}^{3+}$ and $\text{CaSc}_2\text{O}_4:\text{Ce}^{3+}, \text{Nd}^{3+}$ phosphors.

2. Experimental

2.1. Samples preparation

Samples of $\text{CaSc}_2\text{O}_4:\text{Ce}^{3+}$, $\text{CaSc}_2\text{O}_4:\text{Nd}^{3+}$ and $\text{CaSc}_2\text{O}_4:\text{Ce}^{3+}, \text{Nd}^{3+}$ were prepared with co-precipitation method: solutions of $\text{Nd}(\text{NO}_3)_3$ (0.1 mol L^{-1}), $\text{Ce}(\text{NO}_3)_3$ (0.05 mol L^{-1}), $\text{Sc}(\text{NO}_3)_3$ (0.5 mol L^{-1}), $\text{Ca}(\text{NO}_3)_2$ (0.5 mol L^{-1}) were prepared by dissolving the corresponding salts in distilled water. They were mixed with appropriate stoichiometric ratio and added to oxalic acid (1 mol L^{-1}) solution in droplet with stirring. After further stirring for 1 h, the white precipitation was collected, washed four times with distilled water, dried at 110°C for 6 h and sintered at 1300°C for 9 h in a reduced H_2 (5%)– N_2 (95%) atmosphere to get samples.

2.2. Measurements and apparatus

The resultant phosphors were structurally characterized by X-ray diffraction (XRD) (Rigka, D/max-rB analysis with $\text{Cu K}\alpha$ radiation operated at 36 kV and 20 mA, $\lambda = 0.15406 \text{ nm}$, scanning speed $8^\circ/\text{min}$). A scanning electron microscope (SEM, Hitachi, S-3700N) equipped with a EDS components (Bruker, Quantax) was used for elemental analysis. Visible luminescence spectra were measured using a fluorescence spectrophotometer (Hitachi, F-4500) equipped with a 150 W Xenon lamp. NIR luminescence spectra were measured with an optical-fiber spectrophotometer (Model Avaspec-2048). The excitation source was a 150 W xenon lamp equipped with a monochromator. Fluorescence decay curves were recorded with a 500 MHz oscilloscope (Agilent, DSO7054A) and samples were excited with the 337 nm lines from a pulsed N_2 laser (Stanford Research Systems, NL100). All measurements were performed at room temperature.

3. Result and discussion

Fig. 1 shows the XRD patterns of $\text{CaSc}_2\text{O}_4:\text{Ce}^{3+}$ and $\text{CaSc}_2\text{O}_4:\text{Ce}^{3+}, \text{Nd}^{3+}$. Both patterns agree well with Joint Committee on Powder Diffraction Standards (JCPDS) No. 72-1360, indicating that doping of Ce^{3+} and Nd^{3+} do not cause any significant changes in the host structure. CaSc_2O_4 has an orthorhombic crystal structure. Since ionic radii of Ce^{3+} (0.1034 nm)/ Nd^{3+} (0.0995 nm) are similar to Ca^{2+} (0.099 nm), they are expected to occupy the Ca^{2+} site preferentially. The cell parameters calculated from the XRD patterns, as shown in Table 1, show doping of Ce^{3+} and Nd^{3+} results in slightly reducing of the cell parameters, which indicated the presence of cation vacancies in the samples owing to charge compensation which is necessary to replace Ca^{2+} to

Table 1
Cell parameters of samples.

Samples	a	b	c
CaSc_2O_4	9.4550 Å	11.1274 Å	3.1456 Å
$\text{CaSc}_2\text{O}_4:5.0\% \text{Ce}^{3+}, 2.0\% \text{Nd}^{3+}$	9.4538 Å	11.1210 Å	3.1422 Å

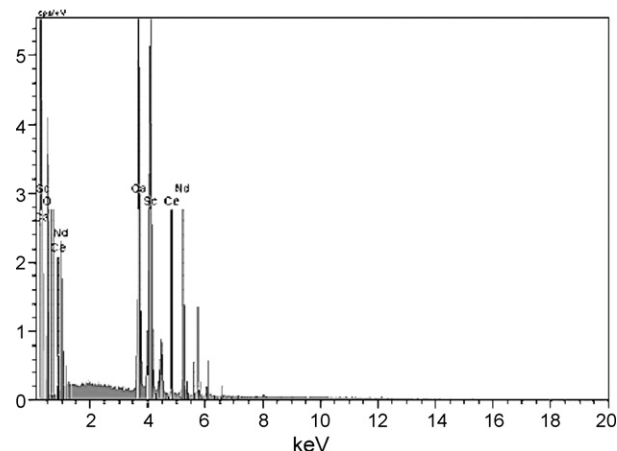


Fig. 2. EDX result of $\text{CaSc}_2\text{O}_4:1.5\% \text{Ce}^{3+}, 2.0\% \text{Nd}^{3+}$.

$\text{Ce}^{3+}/\text{Nd}^{3+}$. EDX measurements also confirm presences of Ce^{3+} and Nd^{3+} in the samples. As a typical case shown in Fig. 2, a Ce^{3+} content of 1.53% and a Nd^{3+} content of 2.02% were found in the $\text{CaSc}_2\text{O}_4:1.5\% \text{Ce}^{3+}, 2.0\% \text{Nd}^{3+}$ sample.

$\text{CaSc}_2\text{O}_4:\text{Ce}^{3+}$ was a recently reported efficient green emission phosphor. The phosphor is very stable in the presence of water, and has great prospect in white LED fabrication [21]. The fluorescence spectra of $\text{CaSc}_2\text{O}_4:\text{Ce}^{3+}$ were shown in Fig. 3. Both the excitation and emission spectra consist of strong single broadband, which originated from the allowed electric-dipole d–f transition of Ce^{3+} ions. The excitation band with peak wavelength of 450 nm matched well with the blue emission of LED based on GaN. The maximum of emission wavelength was found to be 510 nm. Although both emission and excitation spectrum of $\text{CaSc}_2\text{O}_4:\text{Ce}^{3+}$ are slight blue-shift comparing with that of $\text{YAG}:\text{Ce}^{3+}$ [6], the emission spectrum of $\text{CaSc}_2\text{O}_4:\text{Ce}^{3+}$ still overlaps well with the excitation spectrum of Nd^{3+} in CaSc_2O_4 (Fig. 3c). This overlap has been well accepted to be favorable for an efficient energy transfer, similar to the energy transfer from Ce^{3+} to Tb^{3+} in LaPO_4 matrix [20].

Fig. 4 shows the NIR spectra of $\text{CaSc}_2\text{O}_4:\text{Ce}^{3+}, \text{Nd}^{3+}$ and $\text{CaSc}_2\text{O}_4:\text{Nd}^{3+}$. When excited at 450 nm, both $\text{CaSc}_2\text{O}_4:\text{Ce}^{3+}, \text{Nd}^{3+}$ and $\text{CaSc}_2\text{O}_4:\text{Nd}^{3+}$ give characteristic Nd^{3+} emission with similar spectral profile. The Nd^{3+} characteristic emissions consist of three groups of peaks at about 810 nm (${}^4\text{F}_{5/2} \rightarrow {}^4\text{I}_{9/2}$), 880 nm to

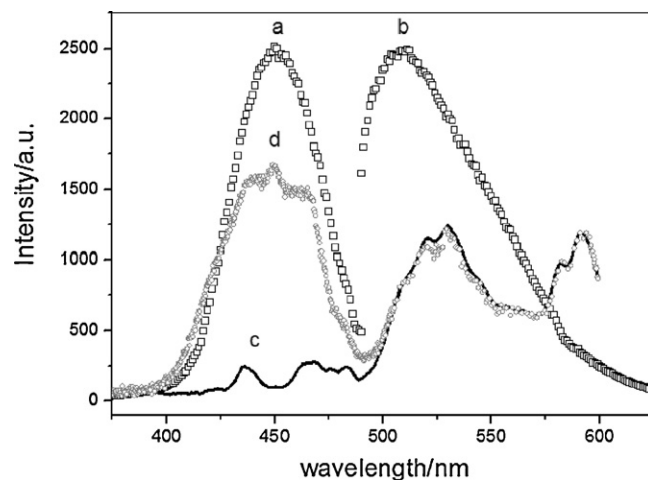


Fig. 3. Fluorescence spectra of $\text{Nd}^{3+}/\text{Ce}^{3+}$ doped CaSc_2O_4 : (a) excitation spectrum of $\text{CaSc}_2\text{O}_4:\text{Ce}^{3+}$ ($\lambda_{\text{em}} = 510 \text{ nm}$); (b) emission spectrum of $\text{CaSc}_2\text{O}_4:\text{Ce}^{3+}$ ($\lambda_{\text{ex}} = 450 \text{ nm}$); (c) excitation spectrum of $\text{CaSc}_2\text{O}_4:\text{Nd}^{3+}$ ($\lambda_{\text{em}} = 890 \text{ nm}$); (d) excitation spectrum of $\text{CaSc}_2\text{O}_4:\text{Ce}^{3+}, \text{Nd}^{3+}$ ($\lambda_{\text{em}} = 890 \text{ nm}$).

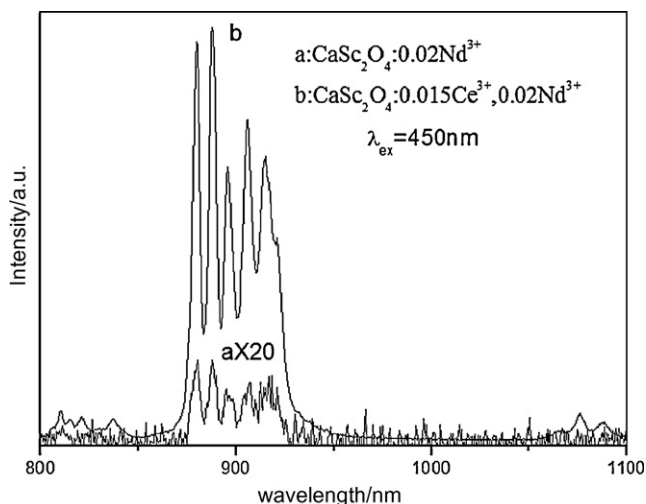


Fig. 4. NIR fluorescence spectrum of $\text{CaSc}_2\text{O}_4:\text{Ce}^{3+}, \text{Nd}^{3+}$ in comparison with that of $\text{CaSc}_2\text{O}_4:\text{Nd}^{3+}$.

930 nm (${}^4\text{F}_{3/2} \rightarrow {}^4\text{I}_{9/2}$), and 1060 nm to 1090 nm (${}^4\text{F}_{3/2} \rightarrow {}^4\text{I}_{11/2}$) [22]. However, their emission intensities are greatly different. The emission intensity of $\text{CaSc}_2\text{O}_4:0.015\text{Ce}^{3+}, 0.02\text{Nd}^{3+}$ at 890 nm is almost 200 times higher than that of $\text{CaSc}_2\text{O}_4:0.02\text{Nd}^{3+}$. These results prompted us to investigate the possible energy transfer from Ce^{3+} to Nd^{3+} in CaSc_2O_4 and develop an efficient NIR phosphor.

Fig. 3c shows the excitation spectrum of $\text{CaSc}_2\text{O}_4:\text{Nd}^{3+}$ when monitored Nd^{3+} NIR emission at 890 nm. All the four peaks can be assigned to the f–f transition of Nd^{3+} ions. The peak wavelengths are 530 nm (strong) (${}^4\text{I}_{9/2} \rightarrow {}^2\text{K}_{13/2} + {}^4\text{G}_{7/2} + {}^4\text{G}_{9/2}$), 592 nm (strong) (${}^4\text{I}_{9/2} \rightarrow {}^2\text{G}_{7/2} + {}^2\text{G}_{5/2}$), 435 nm (weak) (${}^4\text{I}_{9/2} \rightarrow {}^2\text{P}_{1/2}$) and 479 nm (weak) (${}^4\text{I}_{9/2} \rightarrow {}^4\text{G}_{11/2} + {}^2\text{D}_{3/2} + {}^2\text{P}_{3/2} + {}^4\text{G}_{9/2}$) [7,22,23]. The excitation spectrum of $\text{CaSc}_2\text{O}_4:\text{Ce}^{3+}, \text{Nd}^{3+}$ is remarkably different from that of $\text{CaSc}_2\text{O}_4:\text{Nd}^{3+}$ as shown in Fig. 3d. Although the two peaks at 530 and 592 nm mimic well that of $\text{CaSc}_2\text{O}_4:\text{Nd}^{3+}$, the strong band at 450 nm apparently does not originate from the f–f transition of Nd^{3+} ions. Actually, the band position and profile are very similar to the excitation spectrum of $\text{CaSc}_2\text{O}_4:\text{Ce}^{3+}, \text{Nd}^{3+}$ when monitored

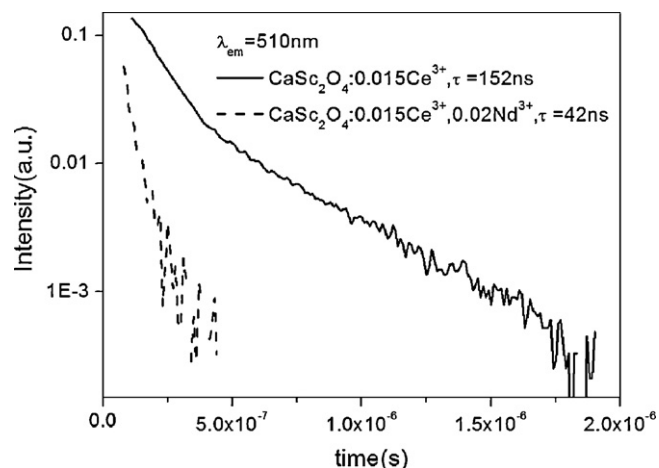


Fig. 6. Fluorescence decay curves of $\text{CaSc}_2\text{O}_4:\text{Ce}^{3+}, \text{Nd}^{3+}$ and $\text{CaSc}_2\text{O}_4:\text{Ce}^{3+}$ monitored at 510 nm.

the visible emission at 510 nm, which corresponds to the emission of Ce^{3+} ions. This similarity indicates that efficient energy transfer from Ce^{3+} to Nd^{3+} take place in the CaSc_2O_4 matrix.

Concentration effects of both Ce^{3+} and Nd^{3+} on luminescence intensity of $\text{CaSc}_2\text{O}_4:\text{Ce}^{3+}, \text{Nd}^{3+}$ phosphors were also investigated as shown in Fig. 5. In CaSc_2O_4 matrix, visible emission of Ce^{3+} at 510 nm is greatly quenched by doping of Nd^{3+} . The energy transfer efficiency can be estimated from the quenching extent of Ce^{3+} emission by doping of Nd^{3+} , which can be calculated from the ratio between fluorescence intensity at 510 nm in $\text{CaSc}_2\text{O}_4:x\text{Ce}^{3+}, 0.02\text{Nd}^{3+}$ and that in $\text{CaSc}_2\text{O}_4:x\text{Ce}^{3+}$ which has a similar Ce^{3+} content with $\text{CaSc}_2\text{O}_4:x\text{Ce}^{3+}, 0.02\text{Nd}^{3+}$. The ratio decreases dramatically with Ce^{3+} concentration as shown in Fig. 5a. This result indicates that quenching of Ce^{3+} emission and energy transfer from Ce^{3+} to Nd^{3+} are both more efficient in samples with higher Ce^{3+} concentration. It is not surprising since energy transfer efficiency is greatly affected by the distance between donor Ce^{3+} ions and acceptor Nd^{3+} ions, and the average distance would reduce with doping concentration. Fig. 5b shows the normalized

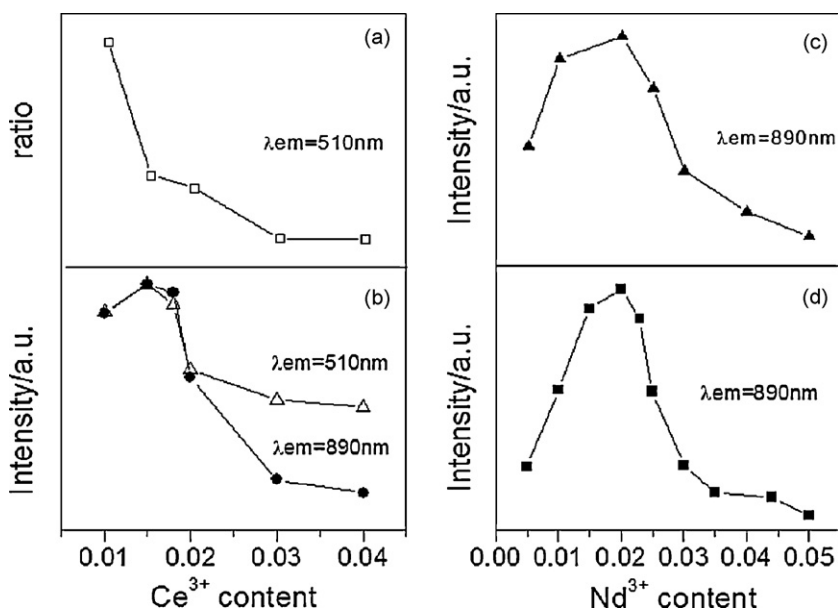


Fig. 5. Effects of doping concentration on emission intensity of $\text{CaSc}_2\text{O}_4:\text{Ce}^{3+}, \text{Nd}^{3+}$ ($\lambda_{\text{ex}} = 450 \text{ nm}$): ratio between fluorescence intensity ($\lambda_{\text{em}} = 510 \text{ nm}$) of Ce^{3+} in $\text{CaSc}_2\text{O}_4:x\text{Ce}^{3+}, 0.02\text{Nd}^{3+}$ and that in $\text{CaSc}_2\text{O}_4:x\text{Ce}^{3+}$ with same x value (a). Normalized NIR fluorescence intensity of $\text{CaSc}_2\text{O}_4:x\text{Ce}^{3+}, 0.02\text{Nd}^{3+}$ in comparison with normalized visible emission of $\text{CaSc}_2\text{O}_4:x\text{Ce}^{3+}$ (b). Effects of Nd^{3+} concentration on NIR luminescence intensity of $\text{CaSc}_2\text{O}_4:\text{Nd}^{3+}$ (c) and $\text{CaSc}_2\text{O}_4:\text{Ce}^{3+}, \text{Nd}^{3+}$ (d).

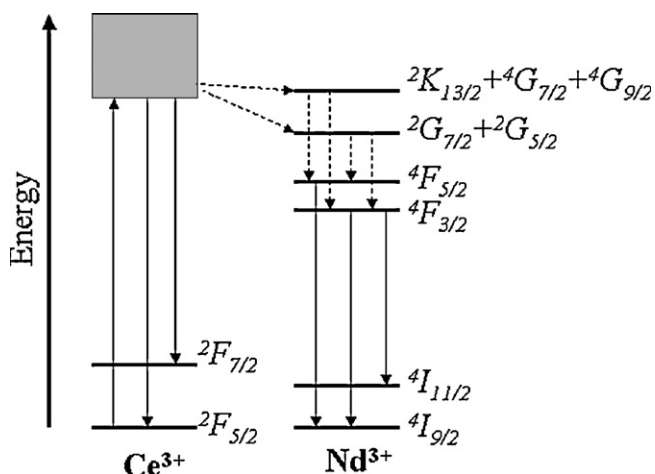


Fig. 7. Energy level diagram which schematizes the energy transfer process from Ce^{3+} to Nd^{3+} in $\text{CaSc}_2\text{O}_4:\text{Ce}^{3+}, \text{Nd}^{3+}$.

NIR emission ($\lambda_{\text{em}} = 890 \text{ nm}$) intensity of $\text{CaSc}_2\text{O}_4:\text{Ce}^{3+}, \text{Nd}^{3+}$ in comparison with the normalized visible emission ($\lambda_{\text{em}} = 510 \text{ nm}$) intensity of $\text{CaSc}_2\text{O}_4:\text{Ce}^{3+}$ phosphors. Both in $\text{CaSc}_2\text{O}_4:\text{Ce}^{3+}, \text{Nd}^{3+}$ and $\text{CaSc}_2\text{O}_4:\text{Ce}^{3+}$ series, samples with $x = 0.015$ give the strongest emission intensity and concentration quenching occurs in higher Ce^{3+} concentration. These results are accordant with the hypothesis that the sensitized Nd^{3+} emission stems from efficient energy transfer from Ce^{3+} . Concentration quenching of Nd^{3+} NIR fluorescence also occurs in samples with high Nd^{3+} concentration, as shown in Fig. 5c and d. Samples with Nd^{3+} concentration of 2.0% give the strongest NIR fluorescence regardless of the presence of Ce^{3+} , which indicates co-doping of Ce^{3+} does not affect concentration quenching effect of Nd^{3+} , and only leads to enhancing of Nd^{3+} NIR emission via energy transfer process.

Fluorescence decay curves of Ce^{3+} were measured as shown in Fig. 6. Fluorescence lifetimes were derived from one order logarithmic curve fitting of the fluorescence decay curves. The lifetime for Ce^{3+} emission at 510 nm is 152 ns in $\text{CaSc}_2\text{O}_4:\text{Ce}^{3+}$, and greatly reduces to 42.0 ns in $\text{CaSc}_2\text{O}_4:\text{Ce}^{3+}, \text{Nd}^{3+}$. The different between the lifetimes is considered to be the result of introducing of acceptor Nd^{3+} ions. An energy transfer efficiency ($\eta(\text{ET})$) of 72% can be estimated through $\eta(\text{ET}) = 1 - k_D/k_{AD}$ [6], with k_D the decay rate in the absence of acceptor (Nd^{3+}) and k_{AD} the decay rate in the presence of acceptor. The energy transfer efficiency for $\text{CaSc}_2\text{O}_4:\text{Ce}^{3+}, \text{Nd}^{3+}$ is slight less than that for $\text{Ce}^{3+}/\text{Nd}^{3+}$ co-doped YAG [7]. The possible explanation is that the Ce^{3+} emission slightly shifts from 515 nm in YAG: Ce^{3+} may match better with excitation spectrum of Nd^{3+} ions, and leads to a more efficient energy transfer. Further studies on other phosphors are still in progress to inspect the effects of the position of Ce^{3+} emission bands on energy transfer efficiency from Ce^{3+} to Nd^{3+} .

An energy transfer mechanism was proposed with a brief energy level diagram as shown in Fig. 7. Excitation of Nd^{3+} occurs mainly via energy transfer from the Ce^{3+} 5d to Nd^{3+} when pumped with blue light. After excitation of the 5d state of Ce^{3+} , a small amount of the electrons can radiatively relax to the Ce^{3+} 4f ground state, producing broadband luminescence in the visible range, while a large amount of electrons transfer to the acceptor levels of Nd^{3+} . The acceptor levels should be $2K_{13/2} + 4G_{7/2} + 4G_{9/2}$ corresponding to the excitation band at 530 nm or $2G_{7/2} + 2G_{5/2}$ corresponding

to the excitation band at 592 nm. Electrons in the acceptor levels further relax through non-radiative decay to $4F_{5/2}$ or $4F_{3/2}$ levels, and then decay to the $4I_{11/2}$ and $4I_{9/2}$ levels, emit at 810, 890 and 1075 nm.

4. Conclusions

A novel NIR emission phosphor, $\text{CaSc}_2\text{O}_4:\text{Ce}^{3+}, \text{Nd}^{3+}$, was synthesized by co-precipitation method. The phosphor gives strong Nd^{3+} characteristic emission at ~ 810 , ~ 890 and $\sim 1075 \text{ nm}$. When irradiated with blue light at 450 nm, a 200 times enhancing of Nd^{3+} characteristic NIR emission can be achieved by co-doping of Ce^{3+} ions. Detailed investigations on spectra and lifetimes indicate the remarkably NIR fluorescence enhancing is obtained from an energy transfer process from Ce^{3+} to Nd^{3+} . Studies on doping concentration effects showed that the energy transfer efficiency increases with Ce^{3+} content and concentration quenching of Nd^{3+} occurred at Nd^{3+} concentration of 2.0% regardless of the presence of Ce^{3+} . The energy transfer mechanism was proposed and briefly discussed. The process initiates with efficient absorption of blue light by Ce^{3+} ions, follow by efficient energy transfer from Ce^{3+} to Nd^{3+} , and emitting strong Nd^{3+} characterized fluorescence. The present high efficient NIR emission phosphor, which is very stable in water solution and can be efficiently excited with a GaN based LED, is believed to have great prospects in bio-label and other techniques.

Acknowledgements

The authors acknowledge the financial support from the Natural Science Foundation of China (Grant no. 30670523), and the Fundamental Research Funds for the Central Universities.

References

- [1] N.S. Li, B.Y. Jiang, J.Z. Hong, G.M. Qing, M. En, Y.P. Chun, Y.Y. Kui, *Micropor. Mesopor. Mater.* 98 (2007) 156–165.
- [2] A. Leleckaite, A. Kareiva, H. Bettentrup, T. Jüstel, H.J. Meyer, *Z. Anorg. Allg. Chem.* 631 (2005) 2987–2993.
- [3] M.H.V. Werts, R.H. Woudenberg, P.G. Emmerink, R.V. Gassel, J.W. Hofstraat, W. Verhoeven, *Angew. Chem. Int. Ed.* 39 (2000) 4542–4544.
- [4] A. D'Aléo, A. Picot, A. Beeby, J.A.G. Williams, B.L. Guennic, C. Andraud, O. Maury, *Inorg. Chem.* 47 (2008) 10258–10268.
- [5] M.H.V. Wefts, J.W. Hofstraat, F.A.J. Geurts, J.W. Verhoeven, *Chem. Phys. Lett.* 276 (1997) 196–201.
- [6] J.X. Meng, K.W. Cheah, Z.P. Shi, J.Q. Li, *Appl. Phys. Lett.* 91 (2007) 151107.
- [7] J.X. Meng, J.Q. Li, Z.P. Shi, K.W. Cheah, *Appl. Phys. Lett.* 93 (2008) 221908.
- [8] M.D. Ward, *Coordin. Chem. Rev.* 251 (2007) 1663–1677.
- [9] B.L. An, J. Song, K.W. Cheah, Y.Y. Ren, Z.X. Cheng, *Inorg. Chim. Acta* 362 (2009) 3196–3200.
- [10] X.L. Li, L.X. Shi, L.Y. Zhang, H.M. Wen, Z.N. Chen, *Inorg. Chem.* 46 (2007) 10892–10900.
- [11] L. Armelao, S. Quici, F. Barigelletti, G. Accorsi, G. Bottaro, M. Cavazzini, E. Tondello, *Coordin. Chem. Rev.* 254 (2010) 487–505.
- [12] C.F. Zhang, H.X. Huang, B. Liu, M. Chen, D.J. Qian, *J. Lumin.* 128 (2008) 469–472.
- [13] R.C. Evans, P. Douglas, C.J. Winscom, *Coordin. Chem. Rev.* 250 (2006) 2093–2126.
- [14] P. Lenaerts, K. Driesen, R.V. Deun, K. Binnemans, *Chem. Mater.* 17 (2005) 2148–2154.
- [15] E.E.S. Teotonio, H.F. Brito, M.C.F.C. Felinto, L.C. Thompson, V.G. Young, O.L. Malta, *J. Mol. Struct.* 751 (2005) 85–94.
- [16] X.M. Shi, R.R. Tang, G.L. Gu, K.L. Huang, *Spectrochim. Acta A* 72 (2009) 198–203.
- [17] Y. Shiraiishi, Y. Furubayashi, G. Nishimura, T. Hirai, *J. Lumin.* 126 (2007) 68–76.
- [18] K. Driesen, R.V. Deun, C.G. Walrand, K. Binnemans, *Chem. Mater.* 16 (2004) 1531–1535.
- [19] M. Yu, J. Lin, J. Fang, *Chem. Mater.* 17 (2005) 1783–1791.
- [20] Y. Qi, J.X. Meng, M. Liu, *Chin. Rare Earths* 27 (2006) 15–18 (in Chinese).
- [21] Y. Shimomura, T. Kurushima, N. Kijima, *J. Electrochem. Soc.* 154 (2007) J234–J238.
- [22] Y. Li, S. Zhou, H. Lin, X. Hou, W. Li, *Opt. Mater.* 32 (2010) 1223–1226.
- [23] M.N. Baranov, E.F. Kustov, V.P. Petrov, *Phys. Stat. Sol.* 21 (1974) K123–K125.